

# Naive Bayes classification model for isotopologue detection in LC-HRMS data

Denice van Herwerden,<sup>\*,†</sup> Jake W. O'Brien,<sup>‡</sup> Phil M. Choi,<sup>¶,‡</sup> Kevin V.

Thomas,<sup>‡</sup> Peter J. Schoenmakers,<sup>†</sup> and Saer Samanipour<sup>\*,†,‡,§</sup>

<sup>†</sup>*Van 't Hoff Institute for Molecular Sciences (HIMS), University of Amsterdam, Amsterdam*

<sup>‡</sup>*Queensland Alliance for Environmental Health Sciences (QAEHS), The University of Queensland, Australia*

<sup>¶</sup>*Water Unit, Health Protection Branch, Prevention Division, Queensland Department of Health, Australia*

<sup>§</sup>*Norwegian Institute for Water Research (NIVA), Oslo, Norway*

E-mail: d.vanherwerden@uva.nl; s.samanipour@uva.nl

## Abstract

Isotopologue identification or removal is a necessary step to reduce the number of features that need to be identified in samples analyzed with non-targeted analysis. Currently available approaches rely on either predicted isotopic patterns or an arbitrary mass tolerance, requiring information on the molecular formula or instrumental error, respectively. Therefore, a Naive Bayes isotopologue classification model was developed that does not depend on any thresholds or molecular formula information. This classification model uses elemental mass defects of six elemental ratios and can successfully identify isotopologues in both theoretical isotopic patterns and wastewater influent samples, outperforming one of the most commonly used approaches (i.e., 1.0033 Da mass difference method - CAMERA).

## 12 Introduction

13 Non-target analysis (NTA) in combination with liquid chromatography high-resolution mass  
14 spectrometry (LC-HRMS) is a comprehensive approach for the characterization of unknown  
15 chemicals in complex sample matrices, originating from, for example, environmental or bi-  
16 ological backgrounds.<sup>1-6</sup> These samples can contain thousands of structurally known and  
17 unknown chemicals. To identify these chemicals, the raw data files need to be processed  
18 to extract and group information that belongs to unique chemical constituents (i.e., parent,  
19 isotopologue, adduct, and (in-source) fragment ions).<sup>1</sup> During this step, one approach to  
20 reduce the number of individual features requiring identification is the detection or removal  
21 of isotopologues (i.e., heavier versions of the same monoisotopic peak).

22  
23 For LC-HRMS data, two main approaches have been used to detect isotopologues.<sup>7,8</sup> The  
24 first strategy relies on a predicted molecular formula, which can be translated to a predicted  
25 isotopic pattern.<sup>7,9</sup> The main shortcoming of this approach is the difficulties associated with  
26 accurate and reliable molecular formula prediction for unknown chemical constituents. The  
27 wrong molecular formula could be assigned to a feature either due to instrumental error or  
28 absence of a chemical constituent in a database. These wrongly assigned molecular formulas  
29 could lead to identifying the potential isotopologues of a feature with the wrong isotopic  
30 pattern, resulting in higher false positive and false negative identification rates.

31  
32 On the other hand, a theoretical mass difference of  $n \times 1.0033$  Da (i.e., CAMERA)  
33 has been used.<sup>8,10</sup> Here  $n$  equals the depth of the isotopologue mass. For example, an  
34 isotopologue mass depth of four corresponds to the mass range of the monoisotopic peak  
35 plus three isotopologues. This approach, even though elegant given that it does not require  
36 information on the molecular formula, does require an arbitrary mass tolerance as input.  
37 This means that the mass tolerance changes, depending on the instrument used, and needs  
38 to be correctly provided by the user.

39

40 In this manuscript, an isotopologue classification model is proposed that requires no  
41 prior knowledge of the molecular composition or arbitrary tolerances. The Naive Bayes  
42 classification model was generated using elemental mass defects, for which the potential in  
43 isotopologue detection was explored. For performance evaluation of the classification model,  
44 a comparison was made with an "in-house" developed mass difference method. This com-  
45 parison was performed for both theoretical isotopic patterns and wastewater influent samples.

46

## 47 **Experimental Section**

### 48 **LC-HRMS Analysis**

49 The forty-four Wastewater influent and three quality control samples were analyzed with  
50 LC-HRMS. Briefly, samples were collected over a time window of 24 hours, using on-site  
51 autosamplers set to use the optimized conditions described by Ort et al.<sup>11</sup> These samples  
52 were filtered, spiked with 10 ng L<sup>-1</sup> of 19 labeled internal standards, and stored frozen until  
53 analysis. For analysis, 10  $\mu$ L of the sample was injected on a biphenyl column at 45°C and  
54 separated using a 10-minute gradient from 5 to 100% methanol with 0.1% formic acid. The  
55 eluent was analyzed using a QToF in positive ion mode with a mass range of 50 to 600 Da  
56 and collision energy of 10 eV. Further details on the analysis are provided elsewhere.<sup>12</sup>

### 57 **Data Processing**

58 The raw data files were converted to mzXML file format, using MSConvertGUI (64-bit, Pro-  
59 teoWizard<sup>13</sup>). Feature lists were generated with the self adjusting feature detection (SAFD)  
60 algorithm, using the following settings: 10 000 maximum number of iterations, a minimum  
61 intensity of 500, resolution of 20 000, 0.02 m/z minimum window size in the mass domain,  
62 0.75 minimum regression coefficient, a maximum signal increment of 5, a signal to noise ratio

63 of 2, and a minimum and maximum peak width in the time domain of 3 and 200 s, respec-  
64 tively.<sup>12</sup> These feature lists were used for the performance evaluation of the classification  
65 model on real samples.

66

## 67 **Theoretical Isotopic Patterns**

68 The isotopic patterns used for setting up the probabilistic isotopologue classification model  
69 were calculated for 737 594 chemicals from the DDS-TOX database.<sup>14</sup> These chemicals con-  
70 sist of a curated list of compounds relevant to environmental and human health. The isotopic  
71 patterns were obtained using pyOpenMS<sup>9</sup> (v2.6.0), combining both the isotopic masses from  
72 the fine<sup>15,16</sup> and coarse<sup>9</sup> isotope pattern generator. The fine isotope pattern generator cal-  
73 culates the hyperfine isotopic pattern that is obtained when the mass defect of isotopes in  
74 taken into account.<sup>9</sup> This mass defect equals the difference between the actual mass of an  
75 atom and the sum of the building blocks (e.g., neutrons) the atom is comprised of. From  
76 this method, isotopologues with a maximum unexplained probability of 0.01% was used.  
77 On the other hand, the coarse isotope pattern generator calculates the unit mass isotopic  
78 patterns, using the summed probability for each isotopologue peak, ignoring the hyper-  
79 fine structures. For this, a maximum isotopic tree depth was required that corresponds to  
80 one plus the maximum number of isotopes that could be present in a single molecule.<sup>16</sup>  
81 Considering the fact that an increasing number of isotopes within a molecule results in a  
82 lower occurrence probability (i.e., intensity), a maximum isotopic tree depth of 6 was chosen.

83

84 The full isotopic pattern for a compound was comprised of the fine and coarse isotopic  
85 patterns, excluding duplicate isotopologues from the coarse isotopic pattern that had a mass  
86 difference of  $\leq$  than 0.003 Da with any of the other isotopologues, which is the typical mass  
87 error observed in LC-HRMS experiments.<sup>17</sup> In this manuscript, a monoisotopic parent ion  
88 with one of its isotopologues is referred to as an mono-iso pair. For example, if a monoiso-

89 topic parent ion has 5 theoretical isotopologues, 5 mono-iso pairs are obtained. In total,  
90 2 691 244 mono-iso pairs were generated, which were employed for training (85% of the  
91 mono-iso pairs) and testing (15% of the mono-iso pairs) of the probabilistic isotopologue  
92 classification model (available on figshare).<sup>18</sup>

93

## 94 **Elemental Ratio Calculations**

95 To construct the probabilistic isotopologue classification model, elemental mass defects  
96 (*EMDs*) were used. The assumption here is that the monoisotopic and isotopologue mass  
97 have the same *EMD* because they have the same molecular structure with the isotopologue  
98 having one or more of its atoms being replaced with heavier versions (i.e., isotopes) of the  
99 same elements. To calculate the *EMD* for both the monoisotopic and isotopologue mass,  
100 the elemental mass (*EM*) needs to be calculated according to equation 1. Here, the *ion<sub>mass</sub>*  
101 can either be the monoisotopic or the isotopologue mass and the *er<sub>mass</sub>* (i.e., elemental ra-  
102 tio mass) depends on the elemental ratio used. For the classification model the elemental  
103 ratios CO, CCl, CN, CS, CF, and CH were used, which have an *er<sub>mass</sub>* of 27.995, 46.969,  
104 26.003, 43.972, 30.998, and 13.008, respectively. These values are the sum of the elemental  
105 masses of each element for a single elemental ratio. For example, the *er<sub>mass</sub>* of CO equals  
106 the monoisotopic mass of a carbon atom plus that of an oxygen atom (i.e., 12.000 + 15.995  
107 = 27.995). The selected elemental ratios were chosen based on both the frequency they  
108 were encountered in the DDS-Tox database (Table S1) and the fact that only 0.007% of the  
109 database entries contain none of the selected elements.

110

111 After the *EM* is calculated, the *EMD* for the monoisotopic and isotopologue mass can  
112 be obtained according to equation 2 (i.e., *EMD<sub>mono</sub>* and *EMD<sub>iso</sub>*, respectively). These *EMD*  
113 values are used to calculate the delta *EMD* (*dEMD*) for an mono-iso pair (Equation 3). It is  
114 important to note that the *EMD<sub>mono</sub>* should always be subtracted from the *EMD<sub>iso</sub>* and not

115 vice versa when using the probabilistic isotopologue classification model described in this  
116 paper. An example case for calculating the  $dEMD$  value can be found in figure 1C. The full  
117 set of isotopologue and monoisotopic  $EMD$  values for the DDS-Tox database can be found  
118 on figshare.<sup>18</sup>

119

$$EM = ion_{mass} \times \frac{rounded\ er_{mass}}{exact\ er_{mass}} \quad (1)$$

$$EMD = roundedEM - exactEM \quad (2)$$

$$dEMD = EMD_{iso} - EMD_{mono} \quad (3)$$

120

121



125 pairs in the training set were used as the true positive cases and true negative cases were  
 126 generated based on the mono-iso pairs from the training set with a randomly added mass  
 127 error between 0.01 to 1 Da to the isotopologue mass. For all mono-iso pairs in the TP  
 128 and TN training set, the *dEMD*s were calculated for the selected elemental ratios (Equation  
 129 3). These *dEMD* values were used to construct the TP and TN probability distributions  
 130 for each of the six elemental ratios. To build these probability distributions, the generated  
 131 *dEMD* values were binned, using a range between -1 and 1 Da with a 0.002 Da step size.  
 132 For each *dEMD* bin, the number of occurrences plus one was used. This prevented that a  
 133 *dEMD* range could have a probability equal to zero, in case no occurrences for that specific  
 134 *dEMD* were found in the training set. Finally, the probability distributions were calculated  
 135 by dividing the occurrence distribution values by the total number of occurrences.

136

## 137 Naive Bayes Classification

138 Naive Bayes classification was used to develop a probabilistic isotopologue detection model,  
 139 using the TP and TN *dEMD* probability distributions obtained for the selected elemental  
 140 ratios (i.e. CO, CCl, CN, CS, CF, and CH). To calculate the posterior probabilities (i.e.,  
 141  $P(A|B)$ ) for classifying a potential mono-iso pair as TP or TN, Bayes theorem is used (Equa-  
 142 tion 4).<sup>19</sup> Here,  $P(A)$  is the probability of an mono-iso pair being TP or TN,  $P(B)$  is the  
 143 occurrence likelihood for a specific *dEMD* value,  $P(B|A)$  is the probability for a *dEMD* value  
 144 in case of A, and n equals the number of elemental ratios used, which would be six for our  
 145 model (i.e., CO, CN, CCl, CS, CF, and CH).

146

$$P(A|B) = \prod_{i=1}^n \frac{P(B|A)_i \times P(A)_i}{P(B)_i} \quad (4)$$

147 Since  $P(B)$  is a marginal probability (i.e., constant probability normalizing factor), equa-

148 tion 4 can be rewritten to equation 5. Additionally, a uniform distribution is assumed for  
149 the prior  $P(A)$ , further reducing the formula to equation 6.

150

$$P(A|B) \propto \prod_{i=1}^n P(B|A)_i \times P(A)_i \quad (5)$$

$$P(A|B) \propto \prod_{i=1}^n P(B|A)_i \quad (6)$$

151 Lastly, for the classification of the potential mono-iso pair, the TP and TN probabilities  
152 are obtained using equation 6. These probabilities were converted to probability percentages  
153 (i.e., on a scale of 0 to 100). Due to the wide range of values that can be obtained for the  
154 TP and TN probabilities, a  $score_{EMD}$  is used instead for the evaluation (Equation 7). Here  
155  $P(TP)$  and  $P(TN)$  equal the true positive and true negative probabilities, respectively. This  
156  $score_{EMD}$  ranges between 1 and minus infinity. In case the potential mono-iso pair has a  
157  $score_{EMD}$  above a set threshold, the potential isotopologue is classified as a correct isotopo-  
158 logue of the monoisotopic ion. An example for the calculation of the  $score_{EMD}$  can be found  
159 in figure 1D

160

$$score_{EMD} = 1 - \frac{P(TN)}{P(TP)} \quad (7)$$

161

162

## 163 Performance Assessment

164 For the performance assessment, the test set was used. In this instance, TN cases were also  
165 generated based on the mono-iso pairs from the test set with a random mass error added  
166 to the isotopologue mass of 0.01 to 1 Da. For both the TP and TN cases, the  $score_{EMDS}$

167 were calculated (Equation 7). To select a suitable  $score_{EMD}$  cut-off value and assess the  
168 performance of the classification model, the TP and false positive (FP) rates were calculated  
169 for a range of  $score_{EMD}$  values. The  $scores_{EMD}$  from 0.7 to 1 Da with a step size of 0.002  
170 Da were employed to calculate the  $TP_r$  and  $FP_r$  (Equation 8 and 9, respectively). Here, the  
171 TPs equal the number of cases from the test set that were correctly classified as an isotopo-  
172 logue, FNs are the number of cases that were incorrectly classified as not an isotopologue,  
173 TNs are cases that were correctly classified as not an isotopologue, and FPs are the that  
174 were wrongly classified as isotopologues.

175

$$TP_r = \frac{TP}{TP + FN} * 100 \quad (8)$$

$$FP_r = \frac{FP}{TN + FP} * 100 \quad (9)$$

176

177

## 178 Mass Difference Method

179 The mass difference method is a commonly used approach for automated isotopologue detec-  
180 tion in LC-HRMS data. This method has already been implemented in different open access  
181 algorithms such as CAMERA and MZmine.<sup>8,10</sup> Here, an "in-house" developed mass differ-  
182 ence strategy was employed to benchmark our classification model against. For the mass  
183 difference method, to assess if a signal is an isotopologue of a monoisotopic peak, first the  
184 mass difference between the signal and monoisotopic ion was calculated. Then, the residue  
185 of the division of the mass difference by 1.0033 Da is obtained. For example, if the mass  
186 difference is 2.0081 Da, the residue would be 0.0015 Da. In case the residue is lower than  
187 the specified mass tolerance, the signal is accepted as an isotopologue of the monoisotopic

188 mass. For the mass difference method, when dealing with the training set a mass tolerance  
189 of  $\pm 0.0001$  Da was used based on the assumption that the theoretical isotopologues do not  
190 contain any mass error. On the other hand for the wastewater samples, this mass tolerance  
191 was increased to  $\pm 0.01$  Da to better reflect the inherent mass error in such data caused by  
192 background signal and instrumental fluctuations.

193

## 194 **Isotopologue Detection Performance for Wastewater Samples**

195 To test the isotopologue classification model on real samples, the isotopologue detection  
196 performance was evaluated for the feature lists obtained from forty-four wastewater influent  
197 samples and three quality control samples. Additionally, a reference compound list com-  
198 prised of forty-five chemicals was used, containing the monoisotopic masses (i.e., protonated  
199 molecular mass), retention times, and parent isotopologue distributions (Table S3). The iso-  
200 topologue distributions for these chemicals were obtained from the isotope pattern preview  
201 tool in MZmine2 (v2.53), using the protonated molecular formula, a minimum intensity of  
202 0.01%, a merge width of 0.0001 Da, and a charge of 1, which showed to cover an isotopologue  
203 mass depth of six.<sup>10</sup>

204

205 The presence of a reference compound was confirmed based on the reference retention  
206 time  $\pm 0.1$  minutes and the monoisotopic parent mass with a mass tolerance of 0.01 Da.  
207 When a reference compound monoisotopic parent mass was present, all features within a time  
208 range of  $\pm 0.1$  minutes were extracted. If a feature’s mass was higher than the monoisotopic  
209 mass and lower than the monoisotopic mass plus  $1.0033 \times 6$  (i.e., isotopologue mass depth  
210 of six), it was evaluated as a potential isotopologue with both the classification model and  
211 the mass difference method. When a model correctly identifies an isotopologue according to  
212 the reference parent isotopologue distribution, it is considered a TP case. Whereas the FP  
213 cases are incorrectly identified isotopologues and the FN cases are the TP cases that were not

214 detected by a model. With these cases, the  $TP_r$  and  $FD_r$  were calculated for the classifica-  
215 tion model and mass difference method (Equation 8 and 10, respectively), which were used  
216 to compare the two isotopologue identification methods.

217

$$FD_r = \frac{FP}{TP + FP} * 100 \quad (10)$$

218

219

## 220 **Calculations and Code Availability**

221 All calculations were performed using a personal computer running Windows 10 Education  
222 with 12 cores and 32 GB of memory. For obtaining the theoretical isotopologues of the DDS-  
223 Tox database Python (v3.9.4) was used and for calculations related to the classification model  
224 Julia (v1.6.0) was used. The mzXML files were imported in julia using the MS\_Import pack-  
225 age, which is available at [https://bitbucket.org/SSamanipour/ms\\_import.jl/src/master/](https://bitbucket.org/SSamanipour/ms_import.jl/src/master/). The  
226 code for the probabilistic isotopologue classification model is available at [https://bitbucket.org/Denice\\_van\\_Leuven/probabilistic\\_isotopologue\\_classification\\_model/src/master/](https://bitbucket.org/Denice_van_Leuven/probabilistic_isotopologue_classification_model/src/master/).  
227 This package includes both the probabilistic isotopologue classification model and functions  
228 to use the model with feature lists obtained either from SAFD<sup>12</sup> or other algorithms. The  
229 code for SAFD is available at <https://bitbucket.org/SSamanipour/safd.jl/src/master/>.

230

## 231 **Results and Discussion**

### 232 **Exploring the EMD probability distributions**

233 Calculating the *EMD* values for the theoretical isotopologues showed that the *EMD* values  
234 for the monoisotopic and isotopologue masses were similar. Figure 2 shows the *EMD* values

235 for the theoretical isotopic distribution of carbamazepine. In this example, a minimum and  
236 maximum absolute difference in  $EMD$  (i.e.,  $dEMD$ ) of 0.003 and 0.020 Da were found, respec-  
237 tively. Additionally, an increase in  $dEMD$  between the  $EMD_{mono}$  and  $EMD_{iso}$  was observed  
238 for isotopologues with a higher isotopologue mass depth. Even though the elements S and F  
239 are not present in the molecular formula of carbamazepine, a similar  $EMD$  trend is observed  
240 as for the elements O, N, CL, and H. On the other hand, figure S1 and S2 show that the  
241 presence of other elements (e.g., Br and P) in the molecular formula also do not influence  
242 the  $EMD$  values.

243

244 Overall, similar trends were observed for all theoretical isotopologue distributions with  
245  $EMD$  values ranging from -0.5 to 0.5 Da for all six elemental ratios. To evaluate this  
246 trend, the Pearson correlation coefficients between the  $EMD_{mono}$  and  $EMD_{iso}$  values were  
247 obtained.<sup>20</sup> These coefficients were calculated separately for each elemental ratio and iso-  
248 topologue mass depth of 1 till 6 (Table S2). The highest correlation of 1.00 was found for  
249 the elemental ratio CN with an isotopologue mass depth of 1 and the lowest value was 0.86  
250 for both the elemental ratios CCl and CS with an isotopologue mass depth of 5 (Figure S3  
251 and S4, respectively). Overall, the Pearson correlation coefficient decreases with a higher  
252 isotopologue mass depth except for an isotopologue mass depth of 6. It is expected that this  
253 was due to a relatively low number of mono-iso pairs with a depth of 6 (Table S2). These  
254 results showed that similar  $EMD$  values for mono-iso pairs were obtained throughout the  
255 theoretical dataset.

256

257 After calculating all  $dEMD$  values for the mono-iso pairs of both the TP and TN cases,  
258 the TP and TN probability percentage distributions were obtained for the selected elemental  
259 ratios (Figure 3). For the TP probability distributions, there were 2 regions for which the TP  
260 probabilities were higher than the TN probabilities. The first region being around a  $dEMD$   
261 of 0, which is in accordance with the hypothesis that the monoisotopic and isotopologue mass

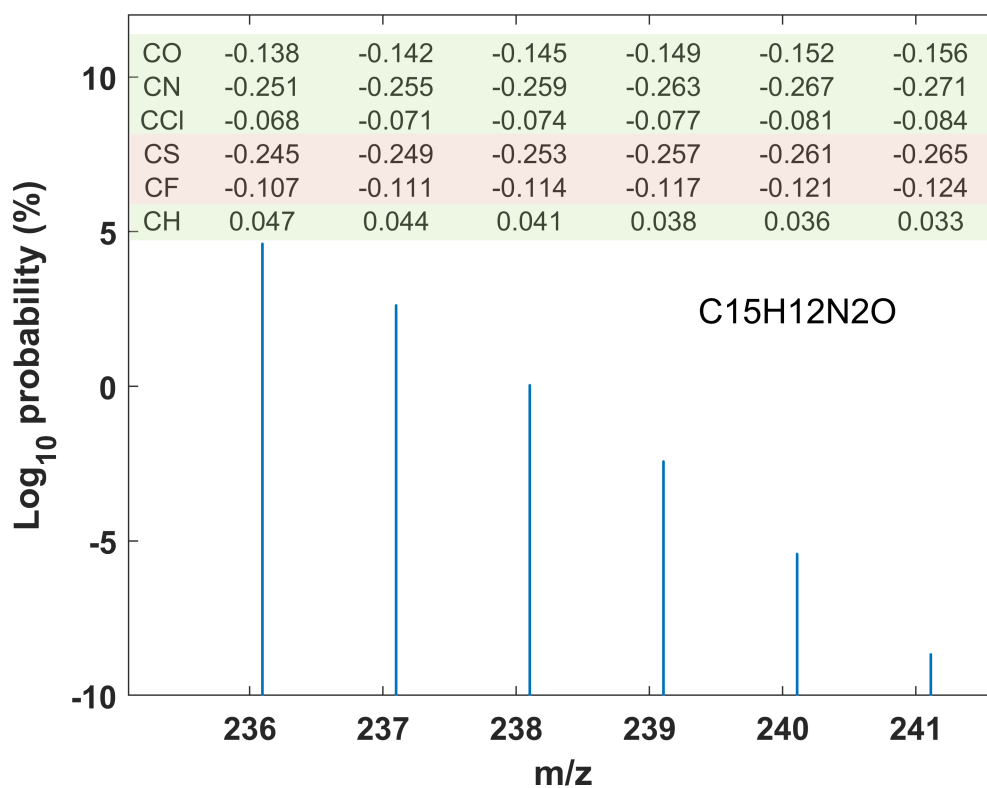


Figure 2: Isotopic distribution of carbamazepine with the corresponding  $\log_{10}$  probability percentages. For the monoisotopic (236.095 Da) and each isotopologue peak (237.098, 238.102, 239.105, 240.108, and 241.112 Da), the *EMD* values are shown above in Da for the elemental ratios CO, CN, CCl, CS, CF, and CH. Additionally, the elemental ratios that are present in the molecule are marked in green and the ones that are not are marked in red.

262 of the same compound obtain similar  $EMD$  values. As for the second region,  $dEMD$  values  
 263 close to 1 and -1 Da were found. For the TN probability distributions, a small decrease  
 264 in probability was observed around a  $dEMD$  of 0 Da, which was caused by the minimum  
 265 added mass error to the isotopologue mass of the TN mono-iso pairs (i.e., 0.01 Da). Overall,  
 266 these plots showed that the  $dEMD$  could be used to differentiate between isotopologue and  
 267 non-isotopologue masses.

268

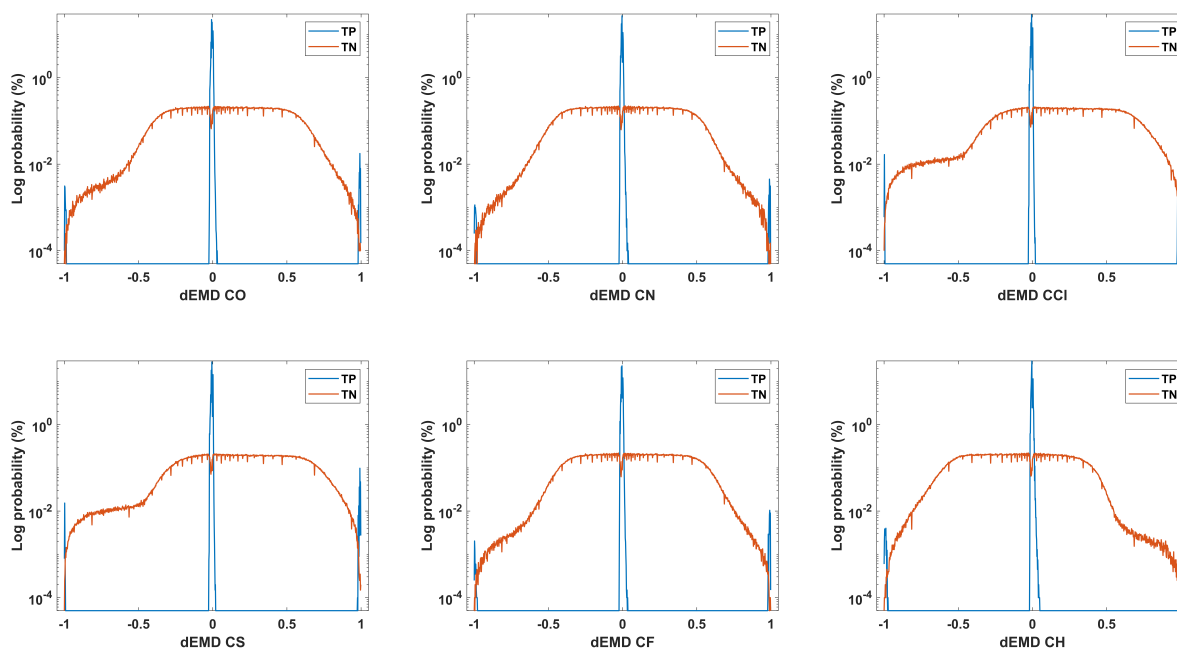


Figure 3: TP and TN probability distributions for the  $dEMD$  values for the selected elemental ratios CN, CCl, CO, CS, CF, and CH.

## 269 Classification Model Performance

270 A receiver operator curve was generated for selection of the  $score_{EMD}$  threshold. This curve  
 271 showed the  $TP_r$  versus the TN rate for  $scores_{EMD}$  between 0.7 and 1 (Figure S5). Based on  
 272 this plot a  $score_{EMD}$  threshold of 0.9997 was selected. This corresponded with a  $TP_r$  and  
 273  $FP_r$  of 99.0 and 1.8%, respectively.

274

## 275 **Comparison with existing method**

276 To evaluate the performance of the classification model with that of the existing mass differ-  
277 ence method, the performance for the in-house mass difference method was evaluated for a  
278 mass tolerance of 0.0001 Da. The mass tolerance was selected based on the assumption that  
279 there is no error present in the theoretical mono-iso pairs and the full receiver operator curve  
280 can be found in sectionS4. For a mass tolerance of 0.0001 Da, a  $TP_r$  and  $FP_r$  of 16.2 and  
281 0.02% was found, respectively. Compared to the results of the classification model (i.e.,  $TP_r$   
282 of 99.0% and  $FP_r$  of 1.8%), both methods performed well with regard to the  $FP_r$  (i.e.,  $\leq$   
283 5%). However, the classification model outperformed the mass difference method for the  $TP_r$ .

284

## 285 **Model Implementation for Real Samples**

286 To evaluate the model performance for real samples, isotopologue detection was performed  
287 for forty-four wastewater influent and three quality control samples. A total of 391 features  
288 were evaluated as potential isotopologues from the forty-fivev reference compounds in ques-  
289 tion. Overall, 212 TP cases, one FN case, and one FP case were found for the classification  
290 model, Resulting in an average  $TP_r$  of 99.8% and an  $FD_r$  of 0.5%. The FN case was caused  
291 by an 0.011 Da mass error between the monoisotopic and isotopologue mass, which is larger  
292 than the minimum mass error (i.e., 0.01 Da) assumed for the true negative cases that are  
293 used for training the model. As for the FP case, the detected isotopologue mass was 155.068  
294 m/z and the monoisotopic parent ion mass was 152.072 m/z. If the decreasing intensity for  
295 less likely isotopologues would have been taken into account, this ion would not have been  
296 included due to the absence of the isotopologues with a higher probability (e.g., 153.068 and  
297 154,075 m/z, Figure S7). From this, it can be concluded that the classification model can  
298 also be used for real data.

299

300 For the mass difference method, a total of 203 TP, 10 FN, and 13 FP cases were found,

301 corresponding to an average  $TP_r$  and  $FD_r$  of 96.3 and 4.8%. For these cases, all FNs were  
302 caused by a mass error larger than 0.01 Da and all FPs were caused by the same reason as  
303 the FP of the classification model. Across multiple datasets a signal at 304.182 m/z was  
304 identified as an isotopologue of codeine, for which the monoisotopic mass was 300.159 m/z.  
305 Only in some cases, an isotopologue at 301.163 m/z was detected, which would still mean  
306 that there were no isotopologues with an isotopologue mass depth of 2 or 3 present with  
307 higher intensities than the signal at 304.182 m/z. To conclude, the classification model had  
308 a higher  $TP_r$  and lower  $FD_r$  than the mass difference method. However, if the decreas-  
309 ing intensity with lower isotopologue probabilities would have been taken into account, the  
310 methods would both have had an  $FD_r$  of 0.0%.

311

## 312 **Potentials and Limitations**

313 The classification model provides a good alternative approach for the detection of isotopo-  
314 logues, requiring no information on the molecular formula or arbitrary thresholds. However,  
315 it should be noted that the classification model is unable to distinguish between isotopo-  
316 logues coming from different chemicals or signals with the same monoisotopic mass. This  
317 would require prior separation such as chromatography. Besides the reduction of total num-  
318 ber of features for identification, correct isotopologue identification can also assist in accu-  
319 rate molecular formula assignment. When multiple formula's are possible for a monoisotopic  
320 mass, the isotopic patterns can be predicted and compared with the detected isotopologues  
321 masses to eliminate less likely candidates. Lastly, the model was built based on isotopic  
322 distributions with a tree depth of six, meaning that it might not be able to correctly classify  
323 ions with more than 6 isotopologues if these ions would be detected at all due to their low  
324 occurrence probabilities. However, if required, the EMDforIso package enables the user to  
325 retrain the classification model using different training sets and parameters.

## 326 Conclusion

327 This manuscript demonstrated the potential of using elemental ratios for the detection of  
328 isotopologues. The classification model that was constructed based on the elemental ratios  
329 CO, CN, CCl, CS, CF, and CH, showed good performance for both theoretical isotopic  
330 patterns as well as real wastewater influent samples. For the theoretical mono-iso pairs,  
331 when assuming no error, the classification model outperformed the mass difference method  
332 with a  $TP_r$  of 99.0% and  $FP_r$  of 1.8% compared to a  $TP_r$  of 16.2% and an  $FP_r$  of 0.02%. As  
333 for the wastewater influent samples, the classification model, with a  $TP_r$  of 99.8% and  $FD_r$   
334 of 0.5%, performed better than the mass difference method, with a  $TP_r$  of 96.3% and  $FD_r$   
335 of 4.8%. However, if a decreasing intensity for a lower probability isotopologue was taken  
336 into account, both methods would have had an  $FD_r$  of 0.0 %.

## 337 Acknowledgement

338 The authors thank the wastewater treatment plants that assisted in the collection of the  
339 wastewater influent samples, the Chemometrics and Advances Separation Team (CAST) for  
340 their insights, and the authors gratefully acknowledge the financial support from the Aus-  
341 tralian Research Council ARC Discovery Project (DP190102476) and Linkage Project(LP150100364).  
342 Finally, the Queensland Alliance for Environmental Health Sciences, The University of  
343 Queensland, gratefully acknowledges the financial support of the Queensland Department of  
344 Health

## 345 Supporting Information Available

346 Information on the presence of the elemental ratios for the chemicals in the DDS-Tox  
347 database, an overview of correlation coefficients for the different elemental ratios between  
348 the  $EMD_{mono}$  and  $EMD_{iso}$  values with scatter plots for the two most extreme correlations,

349 receiver operator curves for the classification model and mass difference method used for the  
350 selection of the *score<sub>EMD</sub>*, a reference compound list used for the performance assessment of  
351 the classification model and mass difference method on wastewater influent samples, and an  
352 example of FP detected isotopologue for the classification model.

## 353 **Author Information**

354 Corresponding Author:

355 Saer Samanipour

356 Van 't hoff institute for molecular sciences (HIMS),

357 University of Amsterdam,

358 the Netherlands

359 Email: s.samanipour@uva.nl

360

361 Denice van Herwerden

362 Van 't hoff institute for molecular sciences (HIMS),

363 University of Amsterdam,

364 the Netherlands

365 Email: d.vanherwerden@uva.nl

366

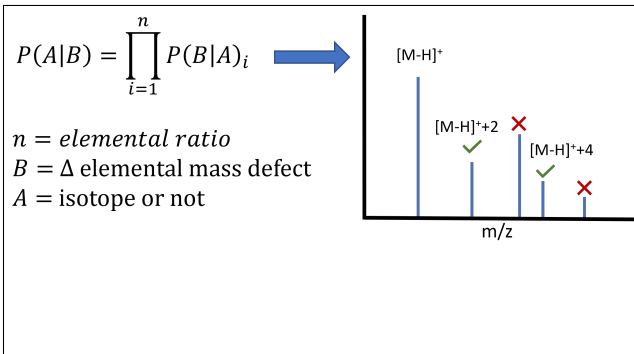
## References

- (1) Bastian, S.; Youngjoon, J.; Sarit, K.; Amy, H. L.; Pradeep, D.; Jake, O.; Maria Jose, G. R.; Sara, G. G.; Jochen, M. F.; Kevin, T. V.; Saer, S. An assessment of Quality Assurance/Quality Control Efforts in High Resolution Mass Spectrometry Non-Target Workflows for Analysis of Environmental Samples. *TrAC Trends in Analytical Chemistry* **2020**, *133*, 116063.
- (2) Schymanski, E. L. et al. Non-target screening with high-resolution mass spectrometry: Critical review using a collaborative trial on water analysis. *Anal. Bioanal. Chem.* **2015**, *407*, 6237–6255.
- (3) Werner, E.; Heilier, J.-F.; Ducruix, C.; Ezan, E.; Junot, C.; Tabet, J.-C. Mass spectrometry for the identification of the discriminating signals from metabolomics: Current status and future trends. *J. Chromatogr. B* **2008**, *871*, 143 – 163, Hyphenated Techniques for Global Metabolite Profiling.
- (4) Samanipour, S.; Reid, M. J.; Bæk, K.; Thomas, K. V. Combining a Deconvolution and a Universal Library Search Algorithm for the Nontarget Analysis of Data-Independent Acquisition Mode Liquid Chromatography-High-Resolution Mass Spectrometry Results. *Environ. Sci. Technol.* **2018**, *52*, 4694–4701.
- (5) Samanipour, S.; Kaserzon, S.; Vijayasarathy, S.; Jiang, H.; Choi, P.; Reid, M. J.; Mueller, J. F.; Thomas, K. V. Machine learning combined with non-targeted LC-HRMS analysis for a risk warning system of chemical hazards in drinking water: A proof of concept. *Talanta* **2019**, *195*, 426 – 432.
- (6) Brack, W.; Hollender, J.; de Alda, M. L.; Müller, C.; Schulze, T.; Schymanski, E.; Slobodnik, J.; Krauss, M. High-resolution mass spectrometry to complement monitoring and track emerging chemicals and pollution trends in European water resources. *Environ. Sci. Eur.* **2019**, *31*, 62.

- 392 (7) Stravs, M. A.; Hollender, J. Open-source workflow for smart biotransformation product  
393 elucidation using LC-HRMS data. *Anal. Chem.* **2017**, *86*, 6812–6817.
- 394 (8) Kuhl, C.; Tautenhahn, R.; Böttcher, C.; Larson, T. R.; Neumann, S. CAMERA: An  
395 integrated strategy for compound spectra extraction and annotation of liquid chro-  
396 matography/mass spectrometry data sets. *Anal. Chem.* **2012**, *84*, 283–289.
- 397 (9) Röst, H. L. et al. OpenMS : a flexible open-source software platform for mass spec-  
398 trometry data analysis. *Nat. methods* **2016**, *13*, 741–748.
- 399 (10) Pluskal, T.; Castillo, S.; Villar-Briones, A.; Orešič, M. MZmine 2: Modular framework  
400 for processing, visualizing, and analyzing mass spectrometry-based molecular profile  
401 data. *BMC Bioinf.* **2010**, *11*.
- 402 (11) Ort, C.; Lawrence, M. G.; Rieckermann, J.; Joss, A. Sampling for pharmaceuticals  
403 and personal care products (PPCPs) and illicit drugs in wastewater systems: Are your  
404 conclusions valid? A critical review. *Environ. Sci. Technol.* **2010**, *44*, 6024–6035.
- 405 (12) Samanipour, S.; O’Brien, J. W.; Reid, M. J.; Thomas, K. V. Self adjusting algorithm  
406 for the nontargeted feature detection of high resolution mass spectrometry coupled with  
407 liquid chromatography profile data. *Anal. Chem.* **2019**, *91*, 10800–10807.
- 408 (13) Chambers, M. C. et al. A cross-platform toolkit for mass spectrometry and proteomics.  
409 *Nat. Biotechnol.* **2012**, *30*, 918–920.
- 410 (14) Grulke, C. M.; Williams, A. J.; Thillanadarajah, I.; Richard, A. M. EPA’s DSSTox  
411 database: History of development of a curated chemistry resource supporting compu-  
412 tational toxicology research. *Computational Toxicology* **2019**, *12*, 100096.
- 413 (15) Lacki, M. K.; Startek, M.; Valkenborg, D.; Gambin, A. IsoSpec: Hyperfast Fine Struc-  
414 ture Calculator. *Anal. Chem.* **2017**, *89*, 3272–3277.

- 415 (16) Loos, M.; Gerber, C.; Corona, F.; Hollender, J.; Singer, H. Accelerated isotope fine  
416 structure calculation using pruned transition trees. *Analytical Chemistry* **2015**, *87*,  
417 5738–5744.
- 418 (17) Alygizakis, N. A.; Samanipour, S.; Hollender, J.; Ibáñez, M.; Kaserzon, S.; Kokkali, V.;  
419 Van Leerdam, J. A.; Mueller, J. F.; Pijnappels, M.; Reid, M. J.; Schymanski, E. L.;  
420 Slobodnik, J.; Thomaidis, N. S.; Thomas, K. V. Exploring the Potential of a Global  
421 Emerging Contaminant Early Warning Network through the Use of Retrospective Sus-  
422 pect Screening with High-Resolution Mass Spectrometry. *Environ. Sci. Technol.* **2018**,  
423 *52*, 5135–5144.
- 424 (18) van Herwerden, D.; Samanipour, S. Dataset for: probabilistic classification model for  
425 isotope detection in high-resolution mass spectrometry. 2021; [https://figshare.com/  
426 articles/dataset/DDS-Tox\\_isotope\\_distributions/16559517/2](https://figshare.com/articles/dataset/DDS-Tox_isotope_distributions/16559517/2).
- 427 (19) Albon, C. In *Machine Learning with Python Cookbook*; Roumeliotis, R., Bleiel, J., Eds.;  
428 O'Reilly Media, Inc., 2018.
- 429 (20) Brereton, R. G. *Applied Chemometrics for Scientists*; John Wiley & Sons, 2007.

430 **Graphical TOC Entry**



431